Effect of graphene oxide addition on the characteristics of nanocomposite films made of graphene oxide and nanocellulose obtained from recycled pulp

Hirsa Jouya
hirsa.jouya@srbiau.ac.ir

*Mohammad Talaeipour**
E-mail: m.talaeipoor@srbiau.ac.ir

Amir Hooman Hemmasi
h_hemmasi@srbiau.ac.ir

Behzad Bazyar
Department of Wood and Paper Science, Faculty of Natural Resources and Environment, Science and Research Branch, Islamic Azad university, Tehran, Iran
bazyar@srbiau.ac.ir

Alain Dufresne
Université Grenoble Alpes, CNRS, Grenoble INP, LGP2, F-38000 Grenoble, France
alain.dufresne@pagora.grenoble-inp.fr

(Received 7 February 2024)

Abstract. Films consisting of 6,6,2,2-tetramethylpiperidine-N-oxyl (TEMPO) oxidized cellulose nanofibers (TOCNFs) prepared from recycled pulp and graphene oxide (GO) were produced by the solution molding method. Electrical conductivity titration and FTIR spectra showed that recycled fibers and cellulose nanofibers were successfully oxidized and the number of carboxyl groups increased. Mechanical properties, thermal stability, crystallinity index, and morphological structure of the nanocomposite films of TOCNFs and GO were characterized by tensile strength tests, thermal gravimetric analysis (TGA), X-ray diffraction (XRD), and scanning electron microscopy (SEM). Tensile strength of films made of TOCNFs with 1.5% GO was 61% higher than those without GO, while tensile strength TOCNF films with 3% GO decreased by 2%. The values did not differ statistically from the non-amended TOCNF. Addition of up to 3% GO did not markedly affect thermal stability of nanocomposite films. Recycled pulp had 83% crystallinity, while the crystallinity index of TEMPO-oxidized cellulose nanofibers decreased to 65.5%. SEM observations showed that TOCNFs and small amounts of GO formed nanocomposite films with a homogeneous structure. This research provides an approach for effective utilization of recycled pulp as a feedstock for cellulose nanofibers and TOCNFs/GO nanocomposite films.

Keywords: Bio-nanocomposite; Cellulose nanofibers; TEMPO-oxidation; Recycled Pulp; Graphene oxide

Introduction

Nanocomposites based on biopolymers, and Nano-scale fillers are of scientific and industrial interest in terms of their biological efficiency and potential for significant performance improvements (Sellinger et al. 1998). Biodegradable nanocomposites are made from biopolymers such as polysaccharides, proteins, and fats. As a renewable, biodegradable, and non-toxic material, cellulose is the most abundant natural polymer on earth. It is produced via photosynthesis at the rate of 10^{11} - 10^{12} t/year (Klemm et al. 2002) and has been used to produce nanocellulose (Turbak et al. 1983). Cellulose nanofibers have attracted a lot of attention in Europe and their cost-effective production is a priority to address a number of environmental issues (Rol et al. 2019). Cellulose nanofibers have distinct features in comparison to cellulose fibers rendering them advantageous for a range of applications including packaging (Lavoine et al. 2012; Saini et al. 2016), printed electronics (Hoeng et al. 2016), papermaking (Bardet et al. 2014; Brodin et al. 2014), composites (Mariano et al. 2014; Oksman et al. 2016), and medicines (Jorfi and Foster 2015).

Cellulose nanofibers have at least one dimension in the nanoscale, have a high specific surface area, and behave like a gel in water. They are transparent and compatible with the

* Corresponding author

environment while retaining unique mechanical and barrier properties. Production of cellulose nanofibers on an industrial scale is possible due to the discovery of methods for reducing energy consumption during mechanical treatment. The energy consumption associated with the manufacturing of cellulose nanofibers utilizing homogenizers, microfluidizers, and grinders is considerable, mostly attributable to the abundance of surface hydroxyl groups that facilitate substantial hydrogen bond interactions among nanofibrils. Over the last decade, several studies have been conducted to decrease energy consumption and enhance the nanofibrillation process (Rol et al. 2019). Two methods have been proposed: new mechanical processes and/or chemical modification of cellulosic fibers. The most common pretreatment method for preparing cellulose microfibrils is TEMPO-oxidation. Oxidation using a 6,6,2,2-tetramethylpiperidine-N-oxyl (TEMPO) mediator includes the conversion of hydroxyl groups into aldehyde and carboxyl functional groups in an aqueous environment at room temperature (Rol et al. 2019).

The main weakness of biopolymer films is their poor mechanical properties and research has been conducted to improve the mechanical properties of polysaccharide-based films (Gontard et al. 1993; Hagenmaier and Shaw 1990; Maftoonazad et al. 2008; Park et al. 1993; Yang and Paulson 2000). Modification of polymers with minerals has been shown to improve polymer properties, including their mechanical strength (Colemanet al. 2006; Han et al. 2011a; Han et al. 2011b). On the other hand, the use of graphene and graphene oxide (GO) in materials research has attracted tremendous attention in various fields, including biomedicine (Feng et al. 2012; Li et al. 2008; Li et al. 2011).

Graphene is an allotrope of carbon consisting of a two-dimensional sheet with SP2 hybridization and a hexagonal lattice structure. Graphene has a variety of mechanical and electrical characteristics that render it well-suited for enhancing the strength of polymer matrices. Several studies have used GO nanosheets or reduced GO to enhance the mechanical or electrical properties of polymers (Salavagione et al. 2009; Steurer et al. 2009; Wu and Liu 2010; Xu et al. 2010). These studies showed that uniform distribution of graphene in the polymer matrix was necessary to obtain the best characteristics.

The large specific surface area of GO has -OH, -COOH, -O- and -C=O functional groups that make it hydrophilic and easily dispersible in water and some organic solvents (Paredes et al. 2008). This makes it simple to fabricate GO sheets using the solution molding technique. Research has shown that GO may be evenly disseminated in a chosen polymer matrix to create graphene oxide-based nanocomposites with superior mechanical and thermal characteristics (Fang et al. 2009; Liang et al. 2009; Villar-Rodil et al. 2009).

Since GO is prepared from inexpensive graphite, it has a tremendous cost advantage over carbon nanotubes, which has encouraged research on polymer/GO composites (He et al. 2012; Rana et al. 2011; Yang et al. 2010).

Feng et al. (2012) produced flexible nanocomposite films consisting of GO and bacterial cellulose and used scanning electron microscopy and X-ray diffraction to show that GO nanosheets were uniformly dispersed in the bacterial cellulose matrix. Furthermore, they found a 10% increase in Young's modulus and a 20% increase in tensile strength in films containing bacterial cellulose, and 5% (wt/wt) gain of GO compared to bacterial cellulose film.

Han et al. (2011) showed that chitosan and GO composite films could be mixed uniformly and that mechanical properties of the composite films, especially in the wet state, increased significantly compared to the chitosan film. These composite films showed a high storage modulus of up to 200°C.

The link between the dispersion state and the reinforcing effect of GO in composite films containing microcrystalline cellulose was examined by Wang et al. (2012) who found that mechanical qualities of composite films were much better than those of the microcrystalline cellulose film and that the strengthening impact of GO and its state of dispersion were closely related.

Yadav et al. (2013) showed that nanocomposite films consisting of sodium carboxymethyl cellulose and 1% GO had had significantly higher tensile strength and Young's modulus than sodium carboxymethylcellulose film alone. Nanocomposite films also showed storage moduli up to 250°C.

Xu et al. (2015) studied the effect of GO on the properties of cellulose nanofibers extracted from banana petiole fibers. They showed that the tensile strength and thermal properties of nanocomposite films were improved when less than 4.4% GO was added.

Zhang et al. (2019) studied the effect of GO and black phosphorus on the physical properties of regenerated cellulose films synthesized from agricultural corn stalk waste. They demonstrated that parenchyma cells derived from maize stem pith could be used to produce regenerated cellulose. Addition of small quantities of GO and black phosphorus to the regenerated cellulose base material improved the performance of regenerated cellulose composite films.

Wang et al. (2018) prepared a composite of GO, chitosan, and cellulose by the phase transfer method. They showed that GO improved the thermal stability of films containing chitosan and cellulose while tensile strength and elongation at break increased in films with low loading levels of GO.

GO has been used as a reinforcement in polysaccharide base materials such as sodium carboxymethyl cellulose (Yadav et al. 2013), bacterial cellulose (Feng et al. 2012), chitosan (Wang et al. 2018), microcrystalline cellulose (Wang et al. 2012) and cellulose nanofibers extracted from banana petiole fibers (Xu et al. 2015). Although a number of studies have been performed on production of cellulose nanofibers from paper pulp, few reports are available on the production of cellulose nanofibers from recycled pulp. The use of TEMPO-oxidized cellulose nanofibers obtained from recycled pulp and their use in the production of nanocomposite films reinforced with GO has not been fully researched.

The objective of this study was to examine the effects of 0.5, 1.5 or 3.0% GO addition on the properties of TOCNFs as the base material to produce nanocomposite films. The mechanical properties and thermal stability of the nanocomposite films of TOCNFs and GO were studied by tensile strength tests and thermogravimetric analysis (TGA).

Materials and methods

Greenfield94 recycled pulp was obtained from the Polytechnic Institute of Grenoble, France, with the specifications listed in Table 1 as cellulose raw material. 6,6,2,2-tetramethylpiperidine-N-oxyl (TEMPO), sodium bromide, sodium hypochlorite solution (15%), hydrochloric acid, and sodium hydroxide were purchased from Sigma-Aldrich and used without further purification. Graphene oxide dry sheets (particle size: 0.2-2 microns) were purchased from Graphene Laboratories (Ronkonkoma, NY, USA). Deionized water was used in all experiments.

TEMPO oxidation of cellulose fibers

Saito's method was used for TEMPO oxidation of cellulose fibers (Saito et al. 2007). Two hundred g of recycled pulp (based on dry weight) was soaked in 10 L of water for 4 hours and then stirred for 5 minutes with an electric stirrer (suspension concentration 0.02 g/mL). TEMPO (1.6 g, with 98% purity) was added and softened with a mortar; 10.3 g sodium bromide (99.5% purity) was added. A 10-15% solution of sodium hypochlorite adjusted to pH 10 with hydrochloric acid and 286.3 g of it was added to the mixture. The suspension was placed in a flask at 25°C with stirring at 200 revolutions per minute for 5 minutes after TEMPO and sodium bromide were added. Sodium hypochlorite was added to the mixture, and 10 L of deionized water were added to produce a concentration to 0.01 g of cellulose/mL. The suspension pH was maintained at 10 by dropwise addition of sodium hydroxide until no reduction was observed, indicating that carboxyl groups were no longer formed and the sodium hypochlorite was completely consumed. The reaction was quenched by lowering the pH to 7 using hydrochloric acid. The suspension was washed with deionized water on a Büchner funnel and a nylon mesh with a hole diameter of 0.65 µm. Figure 1 shows the general pathway of the TEMPO oxidation reaction. The material was resuspended and diluted to 0.02 g/mL using deionized water to produce cellulose nanofibers. The suspension was passed through a grinding machine several times and at certain angles among the disc plates.

Table 1. Specifications of recycled pulp

Mean length-weighted fiber length	859 µm
Mean fiber width	23.7 µm
Macro fibrillation index	0.603%
Fine content, % in length	30.88%

Electrical conductivity titration

The number of carboxyl groups in TEMPO-oxidized cellulose fibers was determined via electrical conductivity titration. Fifteen mg of TEMPO oxidized cellulose fibers were mixed in 200 mL of deionized water in a 500 mL beaker in an ultrasonic bath for 5 minutes. The pH of the suspension was adjusted to 3 using 0.1 M hydrochloric acid (replacing sodium ions with protons). The suspension was titrated by adding 0.2 mL of 0.01 M sodium hydroxide solution. The amount of grafting was calculated in µmol/g with the following formula (da Silva Perez et al. 2003):

$$X = \frac{C \times (V_2 - V_1)}{w} \quad (1)$$

Where X was the amount of carboxyl groups (µmol/g), C was the concentration of sodium hydroxide solution (µmol/L), V_1 corresponded to the presence of an excess amount of strong hydrochloric acid (L), V_2 corresponded to the amount of weak carboxylic acid (L), and was the dry weight of the sample (g).

Production of cellulose nanofibers

After TEMPO-oxidized pre-treatment, the 2% suspension of TEMPO fibers in water was ground in a Matsuko Ultra-fine

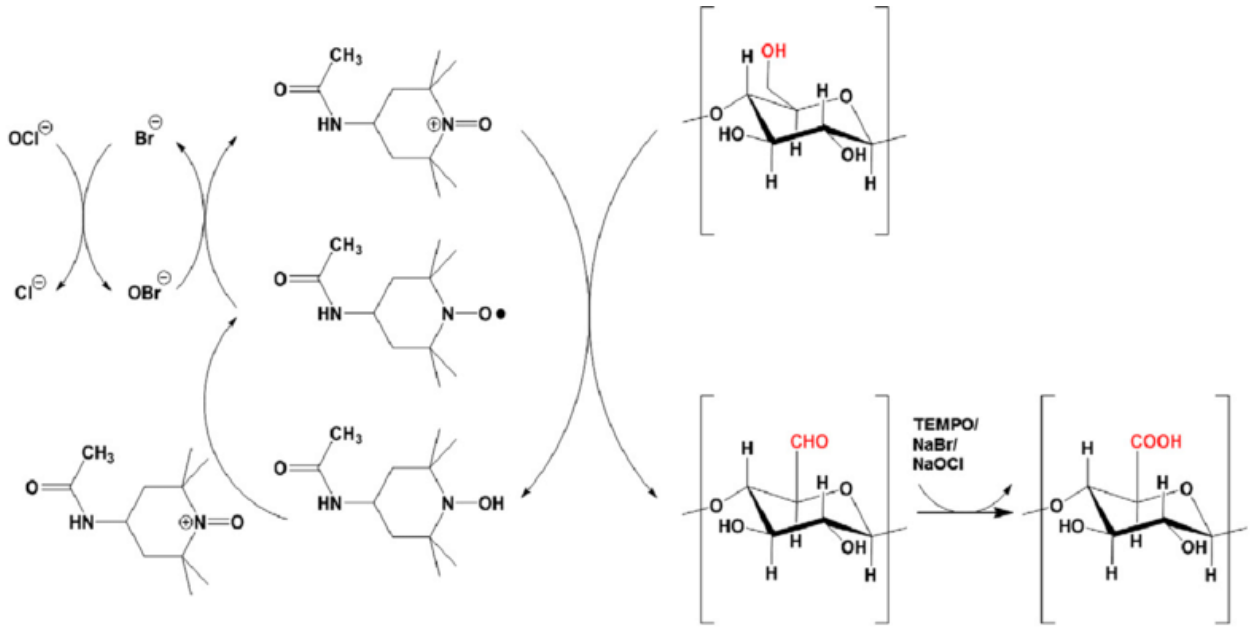

Figure 1. General schematic of TEMPO oxidation (Paquin, Loranger, Hannaux, Chabot, & Daneault, 2013)

friction grinder (Matsuko Sangyo, Honcho, Japan) at 1500 rpm and 32 passes through the grinder (10, 10, 10 and 2 passes, respectively, with the distance between the two discs set between "0", "-5", "-10" and "-20"). This device uses a vertically stacked pair of stone discs. The bottom disk rotates while the top disk remains stationary. The distance between the two discs was modified to a value of -100 µm relative to the initial location of zero displacement prior to the application of the dough. The zero-movement position was determined as the contact position between the two grinder discs before loading the dough. There was no direct contact between two grinding stones, even in the negative setting of the disc position. The resulting suspension of cellulose nanofibers is shown in Figure 2a.

Preparation of TOCNFs/GO nanocomposite films

Nanocomposite films based on TOCNFs containing 0.5, 1.5, and 3 wt% of GO were produced by the solution molding method (Wang et al. 2005). The appropriate amount of suspension of cellulose nanofibers needed to obtain 0.25 g of cellulose nanofibers (based on dry weight) was diluted in deionized water then, 0.000125, 0.00375, and 0.0075 g of GO were mixed in deionized water to prepare films containing 0.5, 1.5, and 3 wt% of GO. The mixtures were subjected to ultrasonic waves in an ultrasonic bath for 15 minutes. Subsequently, the cellulose nanofiber solution was combined with the GO suspension, and 50 ml of deionized water was added. The mixture was blended in an IKA ULTRA-TURRAX homogenizer (IKA Works, Wilmington, NC, USA) for 3 minutes at 7200 rpm, then stirred for 10 minutes while the pH was adjusted to 7 using 0.1 M hydrochloric acid. The mixture was stirred for 1 hr then placed in an ultrasonic bath for 3 minutes to remove the bubbles. The suspension was poured into a Petri dish and oven-dried at 40°C for 24 hr. The thin films of nanocomposite of TOCNFs and GO with an average thickness of 40 µm were characterized (Figure 2b).

Fourier transform infrared spectroscopy (FTIR)

Functional groups of recycled pulp, TEMPO-oxidized cellulose nanofibers, TOCNF/GO nanocomposite films, and graphene oxide were examined using a Bruker Model Vertex 80 FTIR spectrometer (Bruker Inc, Bellerica, MA, USA) equipped with an attenuated total reflection system was used. All sample spectra were collected by accumulating 32 scans from 500 to 4000 cm^{-1}. The background spectrum was collected and subtracted from the original spectrum for each sample.

X-ray diffraction (XRD)

The effects of TEMPO-oxidation pretreatment and mechanical grinding treatment on the crystallinity index of cellulose fibers were investigated by XRD. Recycled pulp, TEMPO-oxidized cellulose nanofibers, TOCNF-GO films and graphene oxide were separately oven-dried at 40°C for 24 hours and powder was prepared from them. Recycled pulp was used as a reference sample. X-ray diffraction spectra were prepared using an XPERT-MDP diffractometer (Malvern Panalytical, Malvern,

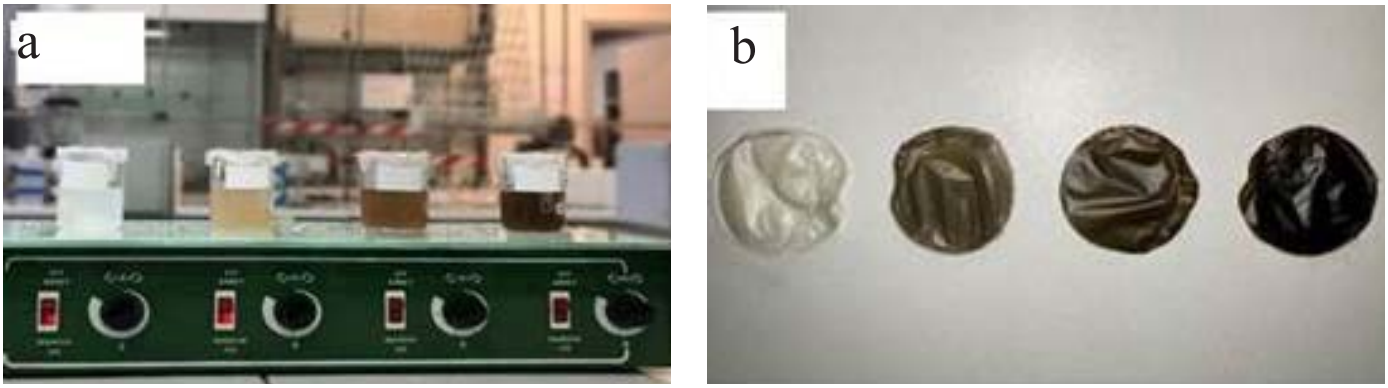

Figure 2. Examples of (a) TOCNFs and TOCNFs/GO suspensions where beaker on the left is TOCNF alone and those to the right containing increasing amounts of GO and (b) TOCNFs/GO nanocomposite films containing 0, 0.5, 1.5 and 3 wt% GO (from left to right, respectively).

United Kingdom) with Cu-Kα radiation at 40 kV and 30 mA at a scan rate of 0.02° s^{-1} over a 2θ scan in the range 10-60°. The crystallinity indices (C.I.) for recycled pulp and TEMPO-oxidized cellulose nanofibers were calculated based on Segal's experimental method (Segal et al. 1959):

$$CI = \frac{I_{002} - I_{AM}}{I_{002}} \times 100 \qquad 2$$

Where I_{002} was the intensity of 002 reflection (2θ between 22° and 23°) and I_{AM} was the minimum value at 2θ between 18° and 19°, which represented the reflection intensity of the amorphous phase.

Scanning electron microscopy (SEM)

Scanning electron microscopic images of oxidized TEMPO nanofibers, and fracture sections of TOCNF/GO nanocomposite films were taken using Field Emission Gun (FEG) SEM, and FEI ESEM QUANTA 200 (Hillsboro, OR USA), respectively. The fracture surface of the films was sputter-coated with gold for better viewing. A drop of a suspension of oxidized TEMPO cellulose nanofibers with a very low solid content, about 10^{-5} %, was placed on a carbon-coated grid and sputter-coated with gold.

Atomic force microscopy (AFM)

A VEECO Nanoscope MultiMode IIIA atomic force microscope (AFM) was used to examine graphene oxide nanosheets. The samples were prepared by depositing a dilute mixture of graphene oxide on the surface of mica and examining the resulting surface.

Transmission electron microscope (TEM)

A Philips Tecnai G2 F20 Transmission electron microscope (TEM) (Philips, Grenoble, France) operating at 200 kV was used to examine graphene oxide nanosheets. GO nanosheets were deposited on a nickel/SiO_2/Si wafer via CVD.

Tensile test

The tensile strength of TOCNF/GO nanocomposite films (5 by 15 mm by nominal thickness of 40 μm) was determined using a SANTAM STM-50 tensile tester (Santam, Teheran, Iran) at a speed of 1 mm/min and a force of 100 N. All the samples were conditioned for 24 hours at 23 ± 5°C and a relative humidity of 50% ± 1% prior to testing. Three samples were evaluated for each film type and values were averaged. The data were subjected to an analysis of variance and means were compared using Duncan's modified least significance test at α = 0.05.

Thermal Gravimetric Analysis (TGA)

Thermal gravimetric analysis (TGA) was performed using a NETSCZH STA 449 C Jupiter simultaneous TG-DSC analyzer (Selb, German). The temperature was increased from room temperature to about 900°C in a nitrogen atmosphere at a rate of 10°C/min. A 10 mg sample was used for each run and the resulting curves were analysed.

Results and discussion

Electrical conductivity titration curves for recycled pulp, TEMPO-oxidized recycled pulp, and TEMPO-oxidized cellulose nanofibers

Electrical conductivity titration curves for recycled pulp, TEMPO-oxidized recycled pulp and TEMPO-oxidized cellulose nanofibers exhibited three separate phases (Figure 3). In the first phase, electrical conductivity decreased in terms of the neutralization of protons (H^+) by hydroxyl ions (OH^-), and the increase of ions (Na^+) which have little mobility. The second phase involved neutralization of carboxylic groups, during which electrical conductivity remained basically unchanged. Sodium ions (Na^+) are absorbed by carboxylic acid groups,

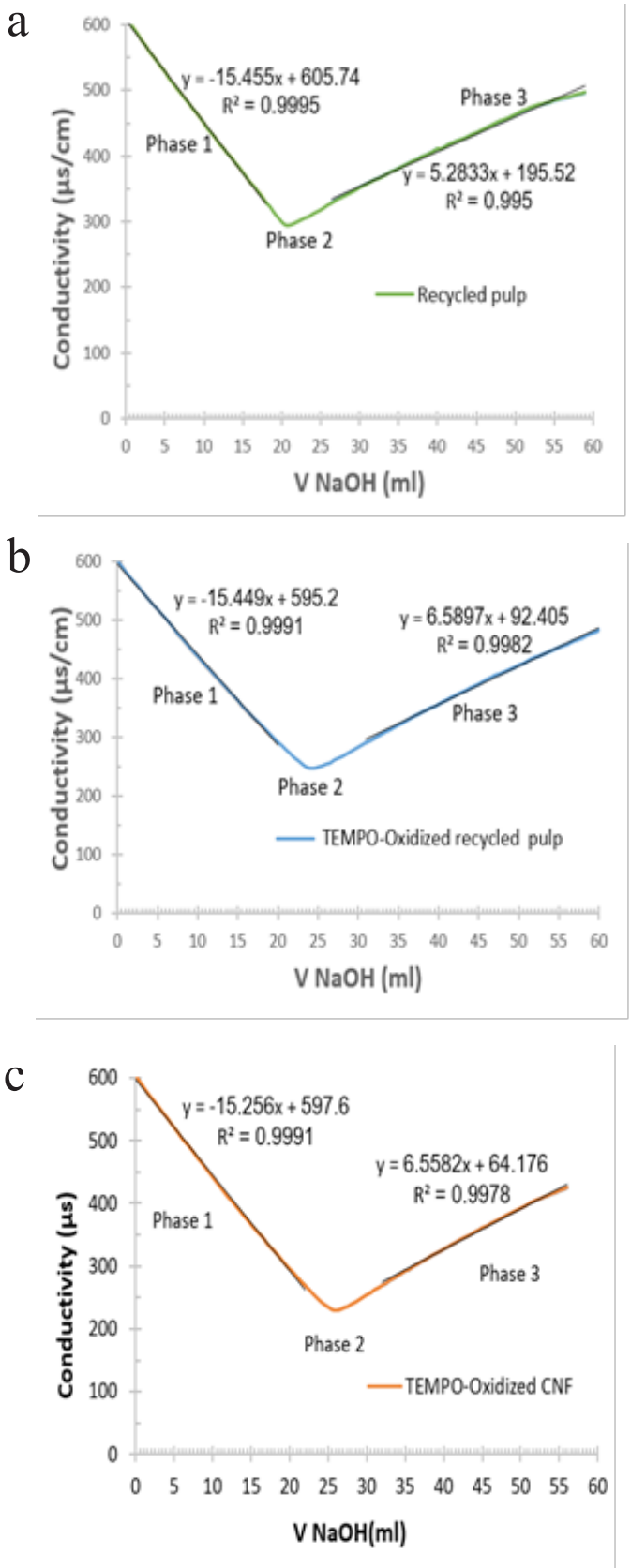

Figure 3. Electrical conductivity titration curves for (a) the recycled pulp, (b) TEMPO-oxidized recycled pulp and (c) TEMPO-oxidized CNF.

and protons (H^+) are neutralized by hydroxyl ions (OH^-). In the third stage, there was an overabundance of sodium hydroxide which increased electrical conductivity. A carboxyl group concentration of around 300 µmol/g is required to create a cellulose nanofiber gel, which may greatly minimize the number of mechanical treatment procedures (Besbes et al. 2011a; Wang et al. 2005). The amounts of carboxylic groups for recycled pulp, TEMPO-oxidized recycled pulp, and TEMPO-oxidized cellulose nanofibers, respectively, were calculated as 117, 975, and 890 µmol/g. The increase in the number of carboxyl groups of TEMPO-oxidized recycled pulp compared to recycled pulp without oxidation confirmed the oxidation of cellulose fibers.

FTIR spectra for recycled pulp, TOCNFs/GO0% film, TOCNFs/GO3% film and graphene oxide

FTIR measurements were used to qualitatively confirm the oxidation level of TEMPO-oxidized cellulose nanofibers. Figure 4 shows the FTIR spectra for recycled pulp, TOCNF/GO0% film, TOCNF/GO3% film, and GO. The absorption peak near 1600 cm^{-1} is related to the C=O stretching vibration of COO^- group. As expected, since the amount of COO^- group in recycled pulp was very low, the absorption peak of 1600 cm^{-1} was more obvious for oxidized cellulose nanofibers than recycled pulp and confirmed the oxidation of cellulose fibers (Benhamou et al. 2014).

Oxygen atoms in GO exist in the form of $-COOH$, $-CO=O$, $-OH$, and $-C-O-C$ groups on the surface or edge of GO sheets and play an important role for improving compatibility between GO and cellulose nanofibers (Wang et al. 2012). Peaks at 1059, 1374.3, 1719.3, 3383.9 and 1621.1 cm^{-1}, respectively, in the GO spectra were attributed to $C-O$ (epoxy or alkoxy functional group), $O-H$ (from carboxyl functional group), C=O (carboxyl and carbonyl functional group), O-H (hydroxyl functional group) and $-C=C-$ functional group (Wang et al. 2012). The absorption peak resulting from the stretching vibration of $O-H$ at 3348 cm^{-1} in nanocomposite films containing 0% or 3% GO decreased compared to recycled pulp. Absorption peaks were also observed at 1600 and 1719 cm^{-1} and are related to stretching vibration of C=O for both TOCNF/GO0%, and TOCNF/GO3%. The reduction of hydroxyl groups appeared to be related to their replacement with carboxyl groups as a result of TEMPO-oxidation. Many oxygen-containing functional groups make GO sheets highly hydrophilic and improve their miscibility in water.

Mechanical properties of TOCNFs/GO nanocomposite films

The mechanical properties of TOCNFs/GO nanocomposite films depend on the uniform distribution of GO in the base

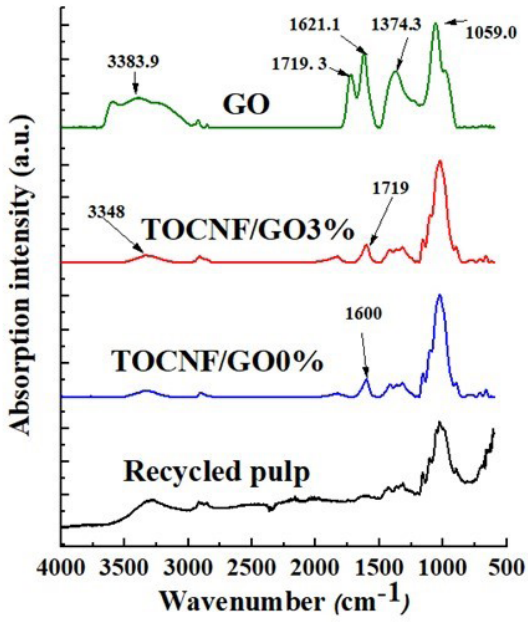

Figure 4. FTIR spectra for recycled pulp, TOCNFs/GO0%, TOCNFs/GO3% and GO.

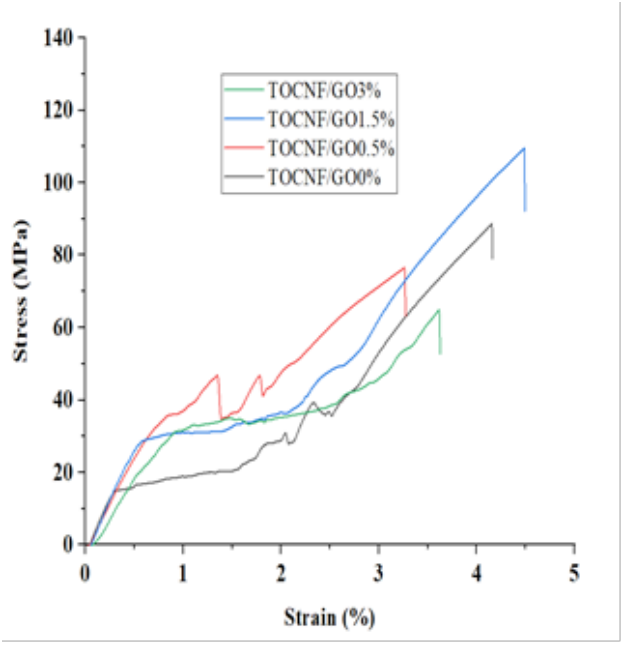

Figure 5. Typical stress-strain curves for TOCNF nanocomposite films with increasing levels of GO.

material of TEMPO-oxidized cellulose nanofibers and the degree of reaction between GO and TOCNFs. Figure 5 shows the stress-strain curves for TOCNFs/GO nanocomposite films. The mechanical properties of TOCNFs/GO nanocomposite films are summarized in Table 2.

Average Young's modulus and tensile strength of TOCNFs/GO0.5%, and TOCNFs/GO1.5% nanocomposite films increased compared to the non-GO amended film (Table 2). The average Young's modulus and average tensile strength of TOCNFs films amended with 1.5% GO were 24% and 61% higher than those obtained for TOCNFs/GO0% film, respectively. The results indicated that proper GO distribution of GO in TOCNFs and the compatibility between TOCNFs and GO contributed to increased film mechanical properties. Oxygen-containing groups in GO can react with TOCNFs through hydrogen. Average Young's modulus and tensile strength for TOCNF/GO3% film were, respectively, 24% and 2% less than those obtained for the none-GO containing TOCNF film. An ANOVA of the data indicated that the addition of GO had no significant effect on either tensile strength or Young's modulus (Table 3).

Table 2. Effect of different levels of GO on mechanical properties TOCNFs/GO nanocomposite films.[a]

GO loading (wt%)	Young's modulus (GPa)	Tensile strength (N)	Elongation at break (%)
0	1.79 (1.11)[a]	10.72 (7.10)	3.80 (0.47)
0.5	2.76 (0.68)	11.08 (3.58)	4.20 (1.85)
1.5	2.22 (0.21)	17.29 (4.29)	5.30 (1.62)
3	1.35 (0.06)	10.50 (2.83)	3.90 (0.91)

a. Values represent means of three replicates while figures in parentheses are one standard deviation.

Table 3. Analysis of variance examining the effect of GO addition on the mechanical strength of nanocomposite films.

	Sum of squares	df	Mean square	F	Sig.
Between Groups	96.348	3	32.116	1.432	0.304
Within Groups	179.481	8	22.435		
Total	275.829	11			

Thermal gravimetric analysis

The thermal stability of nanocomposite films without GO (TOCNFs/GO0%) up to about 300°C was higher than the that of GO (Figure 6). The process of thermal degradation was reversed above 300°C. Thermal degradation of GO slowed above that temperature, but continued for nanocomposite films with or without GO up to 800°C. TGA tests showed that thermal stability of nanocomposite films was better up to 300°C. This could be due to the presence of cellulose nanofibers in the nanocomposite films that imparted TOCNFs with intrinsic resistance to heat. However, thermal degradation of TOCNFs was initiated above 300°C. The addition of up to 3% GO did not greatly affect the thermal stability of the nanocomposite

films. The carbonaceous residue after thermal degradation at 800°C for TOCNFs/GO0%, TOCNFs/GO0.5%, TOCNFs/GO1.5%, and TOCNFs/GO3% nanocomposite films were respectively 12.8%, 15.45%, 15.53%, and 16.35% (Figure 6-c). These observations are consistent with the results of Wang et al. (He et al. 2012), who synthesized composite films consisting of microcrystalline cellulose and GO. They showed that the thermal degradation temperature for the GO films was lower than the pure microcrystalline cellulose film and the amount of carbonaceous residue at 700°C increased compared to the pure microcrystalline cellulose film.

X-ray Diffraction (XRD) Analysis for recycled pulp, TOCNFs, and TOCNFs/GO Nanocomposite Films

XRD spectra for recycled pulp and TOCNFs are shown in Figure 7-a. Compared to the recycled pulp with 83% crystallinity, the crystallinity value of TOCNFs decreased to 65.5%, indicating that the mechanical defibrillation disrupted the crystallites through the breaking effect or peeling-off mechanism of the cellulose chains (Besbes et al. 2011b). Figure 7-b shows the XRD spectra for GO, TOCNFs, and TOCNFs/GO nanocomposite films. The analysis of the XRD spectrum for GO showed an interlayer distance of 0.76 nm, which was within the range of previously reported values (Besbes et al. 2011b; Dubin et al. 2010; Liao et al. 2011). All the XRD spectra for TOCNFs/GO nanocomposite films showed three distinct peaks at $2\Theta = 15.8°$, 22.74°, and 35.0° which were assigned to the $(\bar{1}10)$, (200), and (003) planes, respectively, that indicated the characterization of cellulose I. The XRD spectra for TOCNFs/GO0.5%, TOCNFs/GO1.5%, and TOCNFs/GO3% nanocomposite films were very similar to those of TOCNFs/GO0%, and the diffraction peak corresponding to GO was not

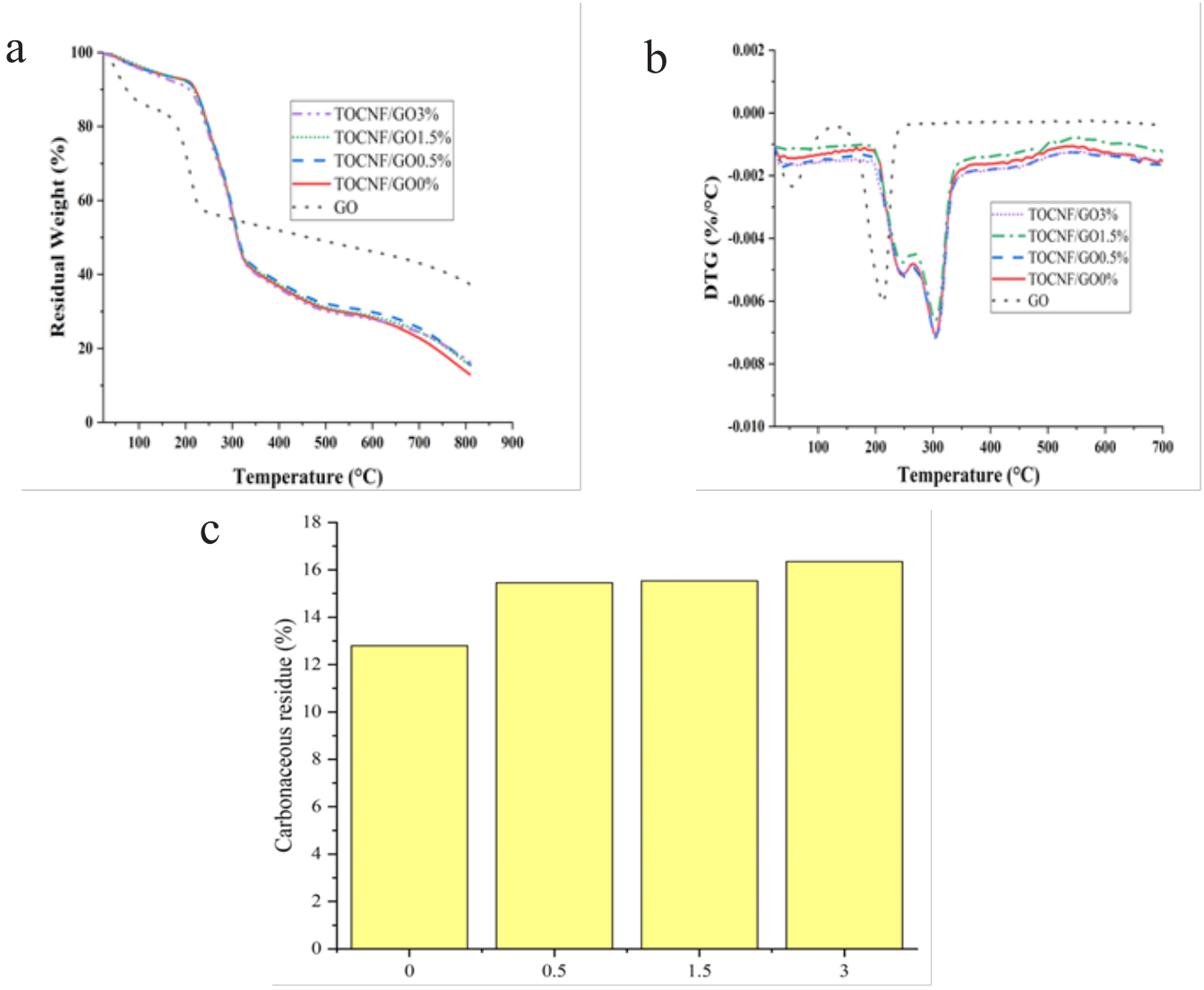

Figure 6. (a) TGA and (b) DTG curves for TOCNFs and TOCNFs/GO nanocomposite films, and (c) carbonaceous residue at 800°C for different levels of GO in the TOCNFs.

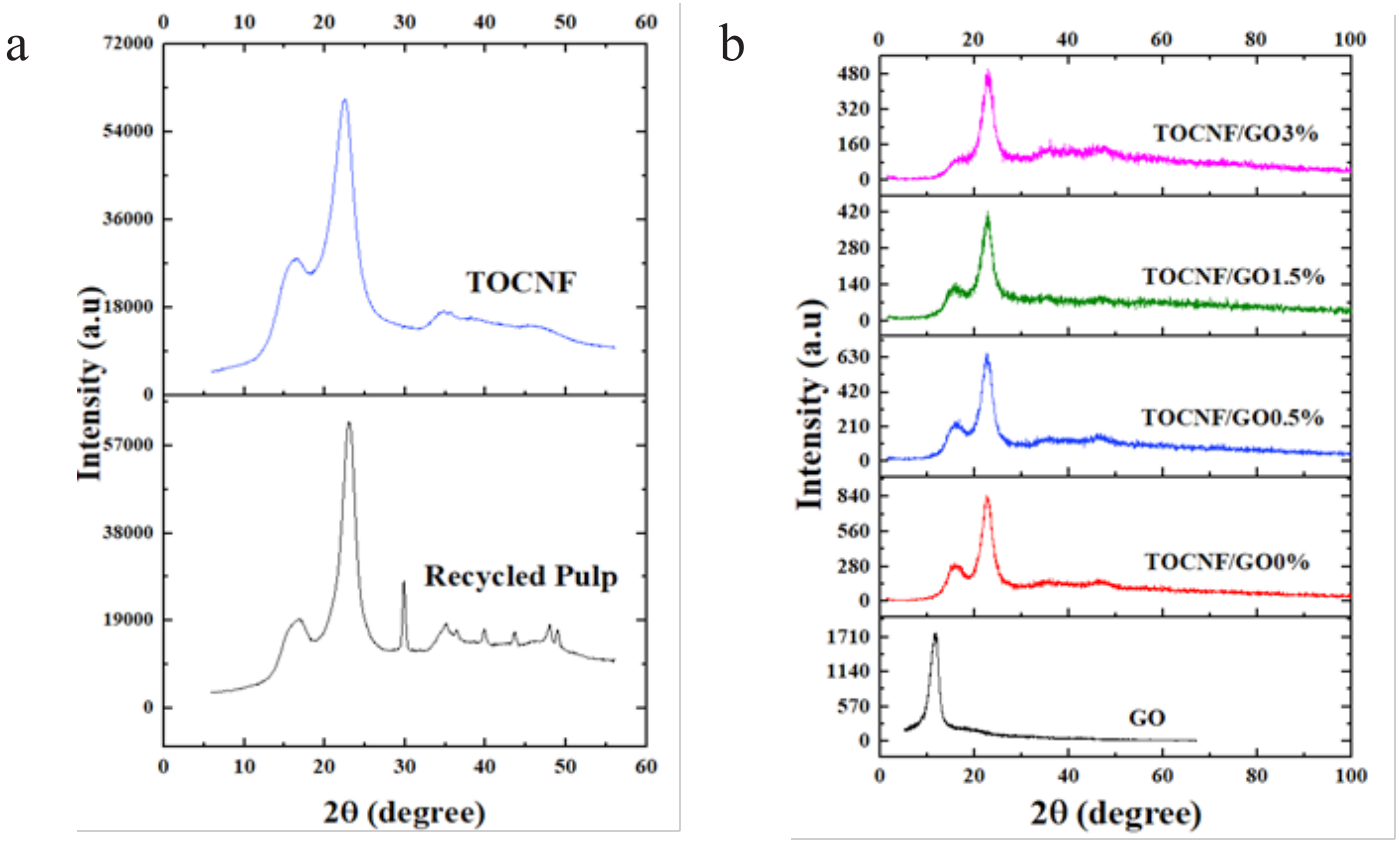

Figure 7. XRD patterns for recycled pulp and TOCNFs (a) and GO, TOCNFs/GO0%, TOCNFs/GO0.5%, TOCNFs/GO1.5%, and TOCNFs/GO3% (b).

observed. The absence of this peak may reflect its low content or possibly efficient exfoliation of GO (Han et al. 2011b) during TOCNFs/GO nanocomposites fabrication.

Morphological analysis

AFM and TEM images from the GO solution confirmed that the purchased GO was almost completely formed into single sheets in the aqueous suspension. Figure 8-a_1, a_2 shows the AFM image of GO and its corresponding height profile on a mica substrate. It shows single sheets of GO with diameters of several hundreds of nanometers and a thickness of 1.1 ± 0.2 nm. A carbon grid was submerged in an aqueous GO solution to create the TEM sample. Figure 8-b shows a TEM image of individual wrinkled GO sheets. Individual GO sheets are important for uniform dispersion in the base material of TOCNFs.

Figure 9a and 9b show FEG-SEM images of TOCNFs produced by TEMPO-oxidization followed by mechanical grinding treatment. SEM images of the cross-section of TOCNFs/GO nanocomposite films are shown in Figure 8c-j. SEM images were taken from the broken surface of samples after the tensile strength test. The fracture surface of the TOCNFs/GO0% film (Figure 9c and 9d) was uniform from the inside to the surface, which indicates a dense and homogeneous texture. However, the fracture surface for TOCNFs/GO 0.5% and TOCNFs/GO 1.5% nanocomposite films (Figure 9-e,f and 9-g,h, respectively) was rougher and without any accumulation of GO, which showed that the GO was uniformly distributed in the TOCNFs matrix. The link between the GO sheets and the TOCNFs was strong enough to allow tension to be transferred between the two components. Furthermore, while GO sheets and TOCNFs had adequate mechanical characteristics on their own, creating a link between them increased the qualities of the resultant composite (Luong et al. 2011). GO sheets and TOCNFs were uniformly mixed in TOCNFs/GO0.5% and TOCNFs/GO1.5% nanocomposite films, and a strong hydrogen bond formed among them. This bonding led to the improvement of mechanical properties of the films. On the other hand, the TOCNFs/GO3% film (Figure 9i and 9j) showed a high accumulation of GO and poor bonding between GO and TOCNFs. This agglomeration led to slippage of the GO sheets and resulted in the lack of stress transfer from the cellulose matrix to the GO sheets. Consequently, this significantly reduced the strengthening ability of the GO (He et al. 2012; B. Wang et al. 2012; Yadav et al. 2013).

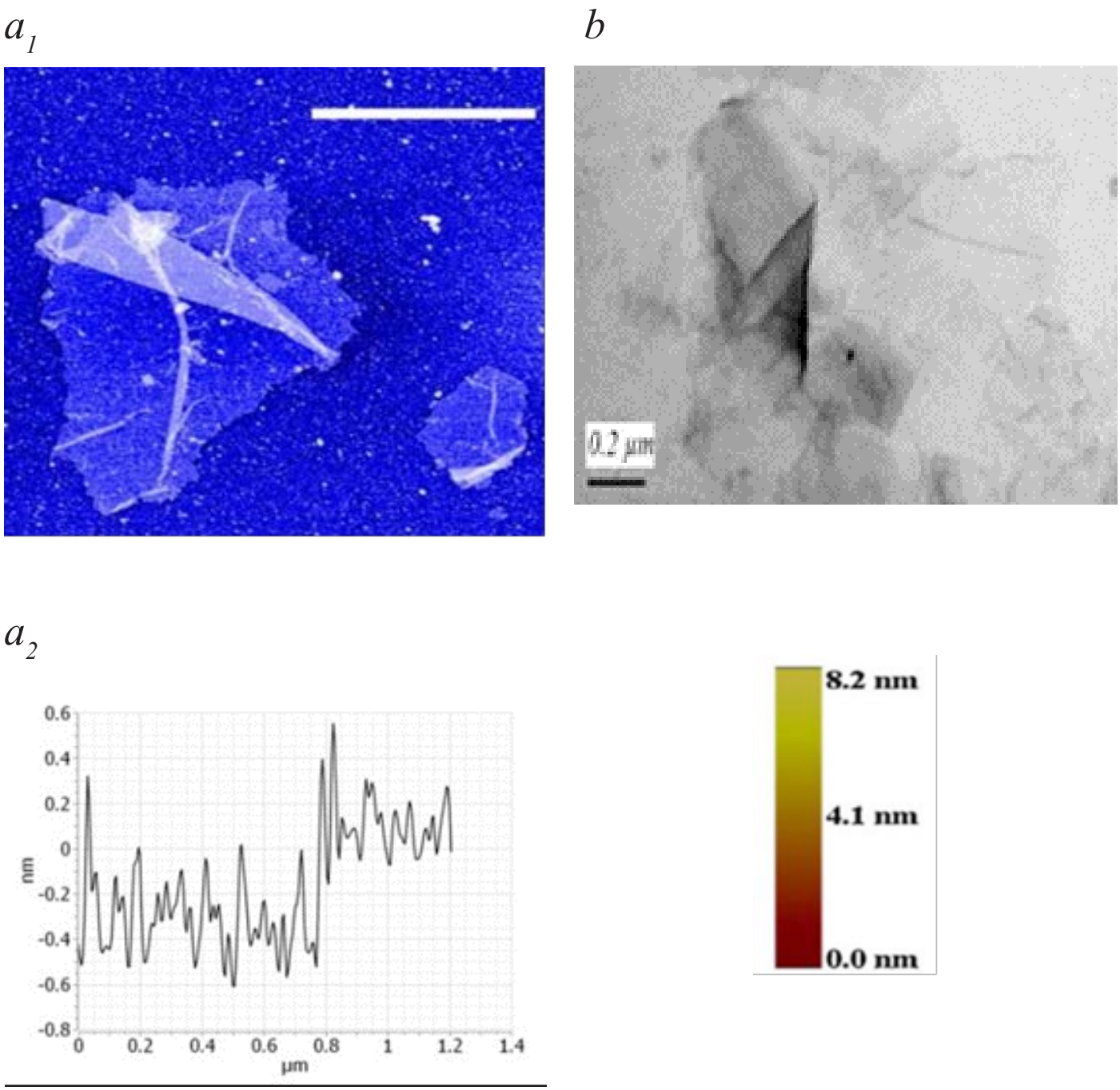

Figure 8. GO sheets shown by (a_1, a_2) AFM with a 1.4 µm scale bar and corresponding height profile and (b) TEM image showing the inclusions of GO sheets, scale bar = 0.2 µm.

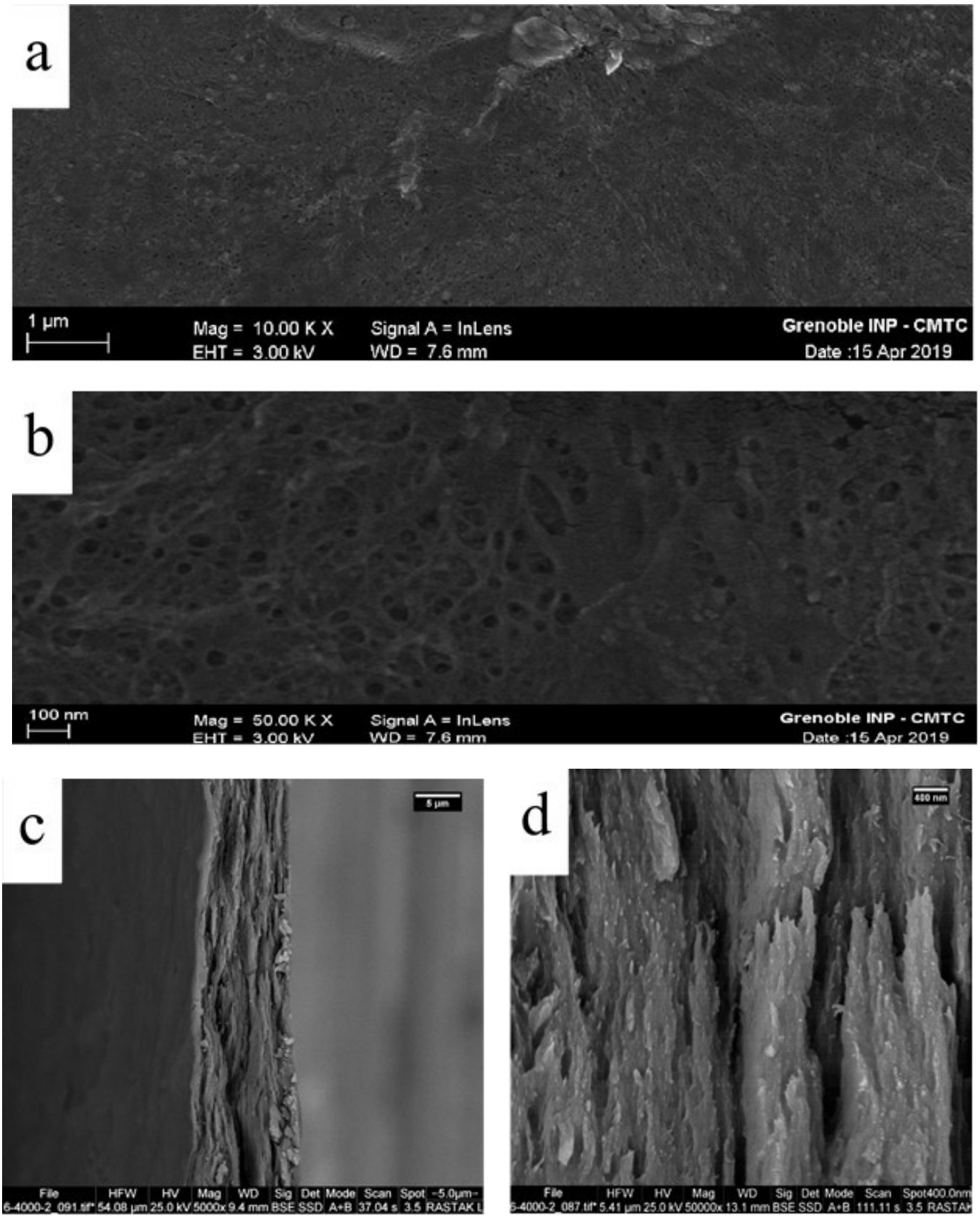

Figure 9. Low and high magnification FEG-SEM images for (a,b) TOCNFs and cross-section SEM images for (c,d) TOCNFs/GO0% composite films, (e,f) TOCNFs/GO0.5%, (g,h) TOCNFs/GO1.5% and (i,j) TOCNFs/GO3% [see following page].

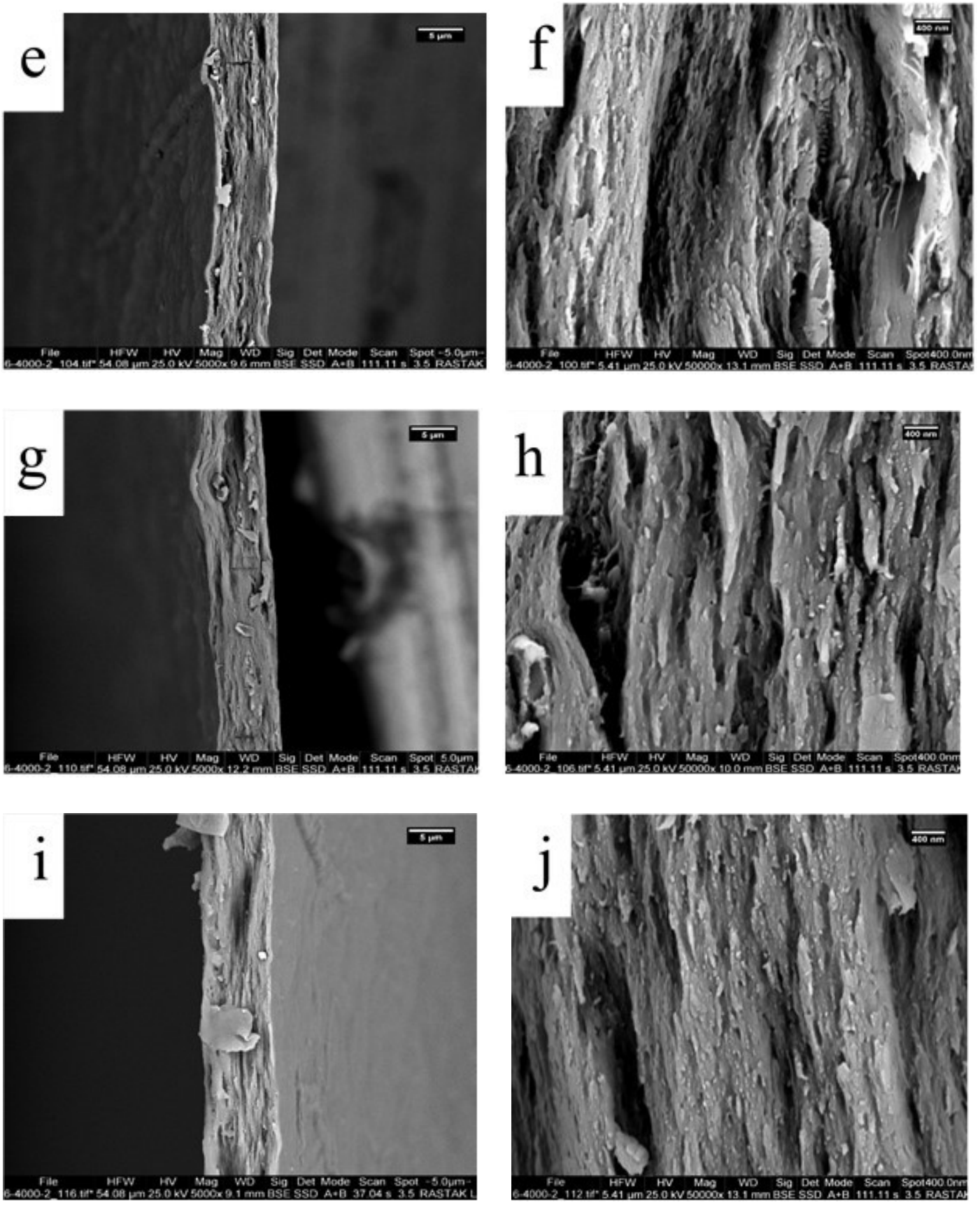

Figure 9 [continued]. Low and high magnification FEG-SEM images for (a,b) TOCNFs and cross-section SEM images for (c,d) TOCNFs/GO0% composite films, (e,f) TOCNFs/GO0.5%, (g,h) TOCNFs/GO1.5% and (i,j) TOCNFs/GO3% .

Conclusion

Nanocomposite films consisting of TOCNFs prepared from recycled pulp, and GO were synthesized via the solution molding method. Electrical conductivity titration and FTIR analysis confirmed that recycled pulp fibers, and cellulose nanofibers were successfully TEMPO-oxidized and the number of carboxyl groups increased. Integration of 1.5% GO resulted in 24% and 61% increases in average Young's modulus and average tensile strength of the TOCNFs/GO films, respectively, compared to a on amended film, but these differences were not significant. Addition of 3% GO resulted in 24% and 2% decreases in average Young's modulus and tensile strength of the TOCNFs/GO films, respectively. TGA results suggested that addition of up to 3% GO did not greatly affect the thermal stability of nanocomposite films. XRD spectrum showed that crystallinity of TOCNFs decreased from 83 to 65.5% compared to the recycled pulp. XRD spectrum of TOCNFs/GO nanocomposite films showed that the GO sheets were exfoliated in the TOCNFs matrix. SEM images illustrated reasonable dispersion of GO in the TOCNFs matrix of TOCNF/GO0.5% and TOCNF/GO1.5% films.

Acknowledgments

The authors would like to thank the Polytechnic Institute of Grenoble, France, and Mr. Naceur Belgacem, the institute's director, for providing the laboratory equipment to conduct the research.

References

Bardet R, Bras J, Belgacem N, Agut P, Dumas J (2014) Method for making paper. WO201411846. 21p.

Benhamou K, Dufresne A, Magnin A, Mortha G, Kaddami H (2014) Control of size and viscoelastic properties of nanofibrillated cellulose from palm tree by varying the TEMPO-mediated oxidation time. Carbohydr Polym 99:74–83.

Besbes I, Alila S, Boufi S (2011a) Nanofibrillated cellulose from TEMPO-oxidized eucalyptus fibres: effect of the carboxyl content. Carbohydr Polym 84(3):975–983.

Besbes I, Vilar MR, Boufi S (2011b) Nanofibrillated cellulose from alfa, eucalyptus and pine fibres: preparation, characteristics and reinforcing potential. Carbohydr Polym 86(3):1198–1206.

Brodin FW, Gregersen ØW, Syverud K (2014) Cellulose nanofibrils: challenges and possibilities as a paper additive or coating material–a review. Nord Pulp Pap Res J 29(1):156–166.

Coleman JN, Khan U, Blau WJ, Gun'ko YK (2006) Small but strong: a review of the mechanical properties of carbon nanotube–polymer composites. Carbon 44(9):1624–1652.

da Silva Perez D, Montanari S, Vignon MR (2003) TEMPO-mediated oxidation of cellulose III. Biomacromolecules 4(5):1417–1425.

Dubin S, Gilje S, Wang K, Tung VC, Cha K, Hall AS, Kaner RB (2010) A one-step, solvothermal reduction method for producing reduced graphene oxide dispersions in organic solvents. ACS Nano 4(7):3845–3852.

Fang M, Wang K, Lu H, Yang Y, Nutt S (2009) Covalent polymer functionalization of graphene nanosheets and mechanical properties of composites. J Mater Chem 19(38):7098–7105.

Feng Y, Zhang X, Shen Y, Yoshino K, Feng W (2012) A mechanically strong, flexible and conductive film based on bacterial cellulose/graphene nanocomposite. Carbohydr Polym 87(1):644–649.

Gontard N, Guilbert S, CUQ JL (1993) Water and glycerol as plasticizers affect mechanical and water vapor barrier properties of an edible wheat gluten film. J Food Sci 58(1):206–211.

Hagenmaier RD, Shaw PE (1990) Moisture permeability of edible films made with fatty acid and hydroxypropyl methyl cellulose. J Agric Food Chem 38(9):1799–1803.

Han D, Yan L, Chen W, Li W (2011a) Preparation of chitosan/graphene oxide composite film with enhanced mechanical strength in the wet state. Carbohydr Polym 83(2):653–658.

Han D, Yan L, Chen W, Li W, Bangal P (2011b) Cellulose/graphite oxide composite films with improved mechanical properties over a wide range of temperature. Carbohydr Polym 83(2):966–972.

He Y, Zhang N, Gong Q, Qiu H, Wang W, Liu Y, Gao J (2012) Alginate/graphene oxide fibers with enhanced mechanical strength prepared by wet spinning. Carbohydr Polym 88(3):1100-1108.

Hoeng F, Denneulin A, Bras J (2016) Use of nanocellulose in printed electronics: a review. Nanoscale 8(27):13131–13154.

Jorfi M, Foster EJ (2015) Recent advances in nanocellulose for biomedical applications. J Appl Polym Sci. 132(14).

Klemm D, Schmauder H, Heinze T, Vandamme E, Steinbuchel A (2002) Polysaccharides II. Polysaccharides from Eukaryotes. Biopolymers 6:275–287.

Lavoine N, Desloges I, Dufresne A, Bras J (2012) Microfibrillated cellulose–its barrier properties and applications in cellulosic materials: a review. Carbohydr Polym 90(2):735–764.

Li D, Müller MB, Gilje S, Kaner RB, Wallace GG (2008) Processable aqueous dispersions of graphene nanosheets. Nat Nanotechnol 3(2):101–105.

Li R, Liu C, Ma J (2011) Studies on the properties of graphene oxide-reinforced starch biocomposites. Carbohydr Polym 84(1):631–637.

Liang J, Huang Y, Zhang L, Wang Y, Ma Y, Guo T, Chen Y (2009) Molecular-level dispersion of graphene into poly(vinyl alcohol) and effective reinforcement of their nanocomposites. Adv Funct Mater 19(14):2297–2302.

Liao KH, Mittal A, Bose S, Leighton C, Mkhoyan KA, Macosko CW (2011) Aqueous only route toward graphene from graphite oxide. ACS Nano 5(2):1253–1258.

Luong ND, Pahimanolis N, Hippi U, Korhonen JT, Ruokolainen J, Johansson LS, Seppälä J (2011) Graphene/cellulose nanocomposite paper with high electrical and mechanical performances. J Mater Chem 21(36):13991–13998.

Maftoonazad N, Ramaswamy HS, Marcotte M (2008) Shelf-life extension of peaches through sodium alginate and methyl cellulose edible coatings. IJFST 43(6):951–957.

Mariano M, El Kissi N, Dufresne A (2014) Cellulose nanocrystals and related nanocomposites: review of some properties and challenges. J Polym Sci B Polym Phys 52(12):791–806.

Nechyporchuk O, Belgacem MN, Bras J (2016) Production of cellulose nanofibrils: a review of recent advances. Ind Crops Prod 93:2–25.

Oksman K, Aitomäki Y, Mathew AP, Siqueira G, Zhou Q, Butylina S, Hooshmand S (2016) Review of the recent developments in cellulose nanocomposite processing. Compos Part A Appl Sci Manuf 83:2–18.

Paquin, M, Loranger É, Hannaux V, Chabot B, Daneault C (2013) The use of Weissler method for scale-up a Kraft pulp oxidation by TEMPO-mediated system from a batch mode to a continuous flow-through sonoreactor. Ultrason Sonochem 20(1):103–108. doi:https://doi.org/10.1016/j.ultsonch.2012.08.007

Paredes JI, Villar-Rodil S, Martínez-Alonso A, Tascon JM (2008) Graphene oxide dispersions in organic solvents. Langmuir 24(19):10560-10564.

Park H, Weller C, Vergano P, Testin R (1993) Permeability and mechanical properties of cellulose-based edible films. J Food Sci 58(6):1361–1364.

Rana VK, Choi MC, Kong JY, Kim GY, Kim MJ, Kim SH . . . Ha CS (2011). Synthesis and drug-delivery behavior of chitosan-functionalized graphene oxide hybrid nanosheets. Macromol Mater Eng 296(2):131–140.

Rol F, Belgacem MN, Gandini A, Bras J (2019) Recent advances in surface-modified cellulose nanofibrils. Prog Polym Sci 88:241–264.

Saini S, Falco ÇY, Belgacem MN, Bras J (2016) Surface cationized cellulose nanofibrils for the production of contact active antimicrobial surfaces. Carbohydr Polym 135:239–247.

Saito T, Kimura S, Nishiyama Y, Isogai A (2007) Cellulose nanofibers prepared by TEMPO-mediated oxidation of native cellulose. Biomacromolecules 8(8):2485–2491.

Salavagione HJ, Gomez MA, Martínez G (2009) Polymeric modification of graphene through esterification of graphite oxide and poly (vinyl alcohol). Macromolecules 42(17):6331–6334.

Segal L, Creely JJ, Martin Jr A, Conrad C (1959) An empirical method for estimating the degree of crystallinity of native cellulose using the X-ray diffractometer. Text Res J 29(10):786–794.

Sellinger A, Weiss PM, Nguyen A, Lu Y, Assink RA, Gong W, Brinker CJ (1998) Continuous self-assembly of organic–inorganic nanocomposite coatings that mimic nacre. Nature 394(6690):256–260.

Steurer P, Wissert R, Thomann R, Mülhaupt R (2009) Functionalized graphenes and thermoplastic nanocomposites based upon expanded graphite oxide. Macromol Rapid Commun 30(4-5):316–327.

Turbak, AF, Snyder FW, Sandberg KR (1983) Microfibrillated cellulose, a new cellulose product: properties, uses, and commercial potential. Paper presented at the J Appl Polym Sci Appl Polym Symp.

Villar-Rodil S, Paredes JI, Martínez-Alonso A, Tascón JM (2009) Preparation of graphene dispersions and graphene-polymer composites in organic media. J Mater Chem 19(22):3591–3593.

Wang B, Lou W, Wang X, Hao J (2012) Relationship between dispersion state and reinforcement effect of graphene oxide in microcrystalline cellulose–graphene oxide composite films. J Mater Chem 22(25):12859–12866.

Wang S-F, Shen L, Zhang W-D, Tong Y-J (2005) Preparation and mechanical properties of chitosan/carbon nanotubes composites. Biomacromolecules 6(6):3067–3072.

Wang S, Gang L, Pu J (2018) Enhancement of the strength of biocomposite films via graphene oxide modification. BioResources 13:6311–6321.

Wu X, Liu P (2010) Facile preparation and characterization of graphene nanosheets/polystyrene composites. Macromol Res 18:1008–1012.

Xu C, Wang G, Xing C, Matuana LM, Zhou H (2015) Effect of graphene oxide treatment on the properties of cellulose nanofibril films made of banana petiole fibers. BioResources 10(2).

Xu J, Wang K, Zu S-Z, Han B-H, Wei Z (2010). Hierarchical nanocomposites of polyaniline nanowire arrays on graphene oxide sheets with synergistic effect for energy storage. ACS Nano 4(9):5019–5026.

Yadav M, Rhee K, Jung I, Park S (2013) Eco-friendly synthesis, characterization and properties of a sodium carboxymethyl cellulose/graphene oxide nanocomposite film. Cellulose 20:687–698.

Yang L, Paulson A (2000) Effects of lipids on mechanical and moisture barrier properties of edible gellan film. Food Res Int 33(7):571–578.

Yang X, Tu Y, Li L, Shang S, Tao X-m (2010) Well-dispersed chitosan/graphene oxide nanocomposites. ACS Appl Mater Interfaces 2(6):1707–1713.